Graphene-assisted spontaneous relaxation towards dislocation-free heteroepitaxy

Sang-Hoon Bae[1,2,10], Kuangye Lu[1,2,10], Yimo Han[3,10], Sungkyu Kim[1,2,10], Kuan Qiao[1,2], Chanyeol Choi [2,4], Yifan Nie[5], Hyunseok Kim [1,2], Hyun S. Kum [1,2], Peng Chen[1,2], Wei Kong[1,2], Beom-Seok Kang[1,2], Chansoo Kim[1,2], Jaeyong Lee[1,2], Yongmin Baek [6], Jaewoo Shim[1,2], Jinhee Park[7], Minho Joo[7], David A. Muller [3,8], Kyusang Lee[6]* and Jeehwan Kim [1,2,9]*

Although conventional homoepitaxy forms high-quality epitaxial layers[1-5], the limited set of material systems for commercially available wafers restricts the range of materials that can be grown homoepitaxially. At the same time, conventional heteroepitaxy of lattice-mismatched systems produces dislocations above a critical strain energy to release the accumulated strain energy as the film thickness increases. The formation of dislocations, which severely degrade electronic/photonic device performances[6-8], is fundamentally unavoidable in highly lattice-mismatched epitaxy[9-11]. Here, we introduce a unique mechanism of relaxing misfit strain in heteroepitaxial films that can enable effective lattice engineering. We have observed that heteroepitaxy on graphene-coated substrates allows for spontaneous relaxation of misfit strain owing to the slippery graphene surface while achieving single-crystalline films by reading the atomic potential from the substrate. This spontaneous relaxation technique could transform the monolithic integration of largely lattice-mismatched systems by covering a wide range of the misfit spectrum to enhance and broaden the functionality of semiconductor devices for advanced electronics and photonics.

The heterointegration of various semiconductors has been of great interest as their dissimilar intrinsic electronic and optical properties can be coupled by the physical stacking of the materials. So far, heteroepitaxy has been one of the most promising methods to integrate dissimilar materials monolithically. However, the formation of crystalline defects such as dislocations in heteroepitaxial layers severely impedes the heterointegration and development of high-performance electronic/photonic devices. To address this challenge, lattice engineering methods such as pseudomorphic and metamorphic heteroepitaxial growth have been developed[12-14]. However, pseudomorphic growth can only be applied for device layers that are grown below a certain critical thickness. Above this critical thickness, dislocations form to relax the built-in strain energy in the epilayers[15-17]. In metamorphic growth, extremely thick graded buffer layers are employed to reduce the dislocation density. However, this strategy cannot completely eliminate dislocations and is inefficient beyond a 2% lattice mismatch, and it substantially

consumes resources for thick and/or complicated buffer schemes[6-8,12,14]. Thus, advanced lattice-engineering solutions must be developed to enable the performance-oriented design of electronic/photonic devices that are not limited by a lattice mismatch between the substrate and device layers.

Here, we demonstrate a lattice-engineering method enabled by inserting an atomically thin graphene layer in between the epitaxial layer and the substrate; this graphene layer allows the heteroepitaxy of the highly lattice-mismatched system with a substantially reduced dislocation density. We discover that once heteroepitaxy is performed on graphene-coated substrates, a single-crystalline epitaxial film is obtained, as the remote interaction through the graphene helps atomic registry guidance[18], while the attenuated binding energy between the epilayer and the substrate allows the spontaneous relaxation of the misfit strain in the epitaxial film grown on the graphene. Thus, we demonstrate that the weakened interface energy offers an alternative pathway for strain relaxation during heteroepitaxy on graphene-coated substrates, while conventional heteroepitaxy relaxes the accumulated strain energy in lattice-mismatched films via the introduction of threading dislocations to form misfit dislocations. We studied systems with a small lattice mismatch (InGaP on GaAs with 0.74% mismatch) and large lattice mismatch (GaP on GaAs with 3.7% mismatch). Density functional theory (DFT) calculation confirms that the energy required for interface displacement on graphene is much lower than the energy required for introducing a dislocation, indicating that the strain can be relieved at the slippery graphene surface before reaching a threshold energy level to introduce misfit dislocations. This result clearly proves the potential of employing spontaneous relaxation to mitigate dislocation formation in lattice-mismatched systems; thus, it will motivate advances in electronic and photonic devices that were previously not possible due to the strict lattice-matching rule for conventional epitaxy.

We attempted to study the relaxation behaviour of strained heteroepitaxial films grown on lattice-mismatched substrates with and without a graphene interlayer. To track intermediate relaxation, we began by exploring a system with a small lattice mismatch (0.74%) by growing $In_{0.4}Ga_{0.6}P$ films on GaAs substrates, thus avoiding
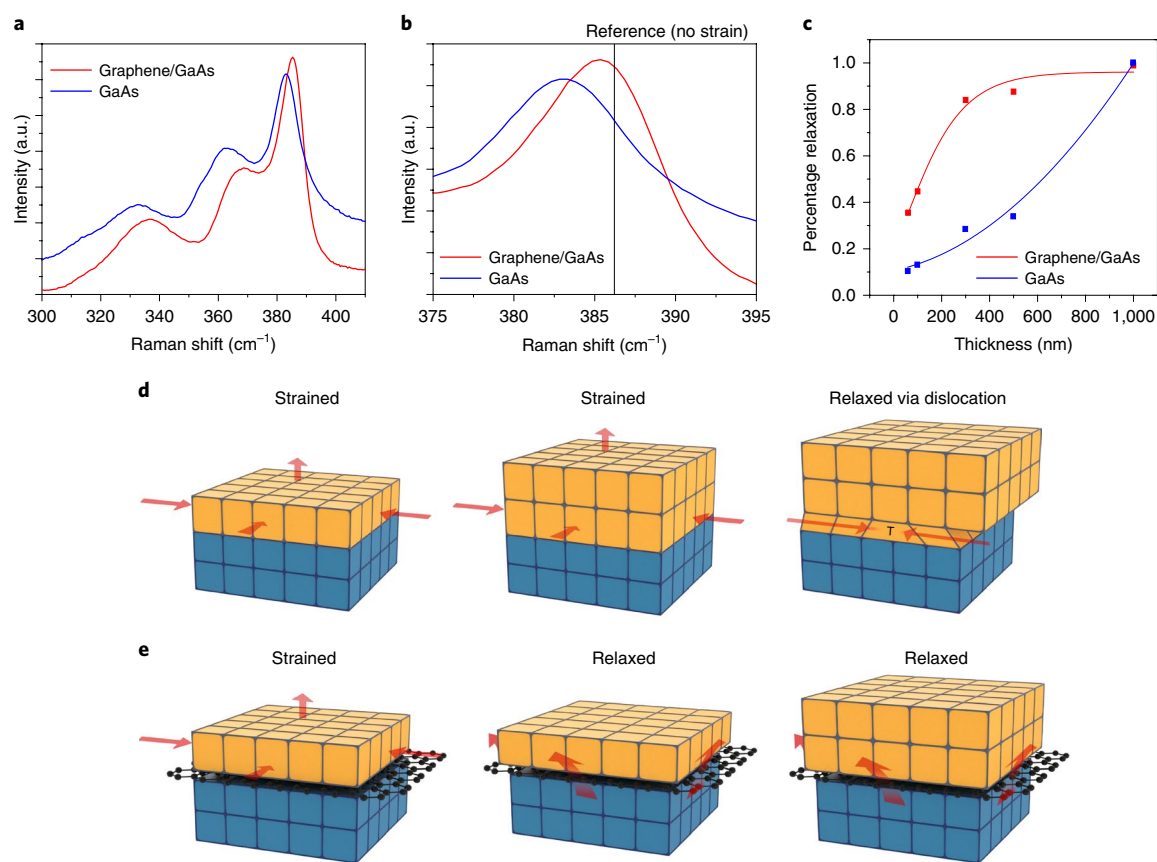
Fig. 1 | Strain analysis by Raman spectra and schematic images. a,b, Raman spectra on InGaP with 0.74% tensile strain, grown on graphene/GaAs and on bare GaAs. **c**, Strain-relaxation efficiency of InGaP grown on graphene/GaAs and on GaAs. InGaP grown on graphene/GaAs shows abrupt relaxation while InGaP grown on GaAs shows gradual relaxation as the accumulated strain energy increases. **d**, Schematic diagram of strain relaxation via the introduction of a dislocation. T indicates where a dislocation forms. **e**, Schematic diagram of strain relaxation via spontaneous relaxation.

immediate strain relaxation. As the remote interaction of III–V materials is only guaranteed through monolayer graphene, we confirmed the monolayer thickness of the graphene transferred on the GaAs substrates with Raman spectroscopy (Supplementary Figs. 1 and 2)[19]. We investigated the strain relaxation of 300-nm $In_{0.4}Ga_{0.6}P$ films grown on a GaAs substrate with and without a monolayer graphene interlayer by measuring the Raman spectra of the $In_{0.4}Ga_{0.6}P$ films. The Raman spectra of $In_{0.4}Ga_{0.6}P$ show a clear difference in peak positions between samples with epitaxy on graphene-coated substrates and those on bare substrates. From the reference longitudinal optical (LO) peak of fully relaxed $In_{0.4}Ga_{0.4}P$ (386 cm^{-1}), the peak of $In_{0.4}Ga_{0.6}P$ grown on graphene/GaAs is shifted by 0.75 cm^{-1}, which corresponds to a tensile strain of 0.15%. However, the peak of $In_{0.4}Ga_{0.6}P$ grown directly on GaAs is further shifted by 2.41 cm^{-1}, which corresponds to a 0.5% tensile strain[20–23]. Thus, $In_{0.4}Ga_{0.6}P$ grown on graphene/GaAs is substantially relaxed by 78%, whereas $In_{0.4}Ga_{0.6}P$ grown directly on GaAs is relaxed by 30% (Fig. 1a,b). This result motivated us to further study the relaxation behaviour of the samples with/without graphene as a function of the thickness of the epitaxial films, since the accumulated strain energy increases as the film gets thicker. As shown in Fig. 1c, $In_{0.4}Ga_{0.6}P$ grown directly on GaAs shows a gradual increase in relaxation as a function of thickness. However, $In_{0.4}Ga_{0.6}P$ films grown on graphene/GaAs relaxed spontaneously, signifying that the degree of relaxation is greater than that of heteroepitaxial $In_{0.4}Ga_{0.6}P$ on GaAs even when the films are 40 nm thick. It is well known that the relaxation pathway of strained epitaxial films for heteroepitaxy is by the introduction of a dislocation, as shown in Fig. 1d. Our findings imply

that an alternate relaxation pathway exists, as hypothesized in Fig. 1e, where the misfit strain can be immediately relaxed on the graphene surface.

Such relief of misfit strain on graphene was directly observed by cross-sectional transmission electron microscopy (TEM) to confirm the relief of the misfit strain. Annular dark-field scanning TEM (ADF-STEM) shows a direct covalent interface between the epilayers and the substrates for a direct heteroepitaxial sample (Fig. 2a). On the other hand, scanning transmission electron microscopy (STEM) reveals the van der Waals gap of the graphene-coated samples (Fig. 2b), where the graphene is not clearly visualized owing to a non-ideal tilt angle as well as interface roughness. Electron energy loss spectroscopy analysis reveals the clear existence of graphene at the interface as shown in Supplementary Fig. 3, implying a non-damaged interface. STEM geometric phase analysis (GPA) scans the difference in the lattice constant of InGaP compared with that of GaAs as e_{xx} for the horizontal direction and e_{yy} for the vertical direction, which directly confirms the clear differences in the relaxation of the $In_{0.4}Ga_{0.6}P$ films with/without a graphene interlayer. As shown in Fig. 2c, 300-nm $In_{0.4}Ga_{0.6}P$ films grown directly on GaAs show as pseudomorphic films with rectangular lattices with a smaller aspect ratio, implying that the $In_{0.4}Ga_{0.6}P$ film is still strained due to a lattice mismatch. On the other hand, 300-nm $In_{0.4}Ga_{0.6}P$ films grown on graphene/GaAs show lattices close to cubic, implying substantial relaxation of the InGaP lattice (Fig. 2d). To examine the relaxation analysis based on GPA maps more quantitatively, we plotted the aspect ratio of InGaP as a function of % relaxation (see Supplementary Fig. 4 for the calculation process as well as the
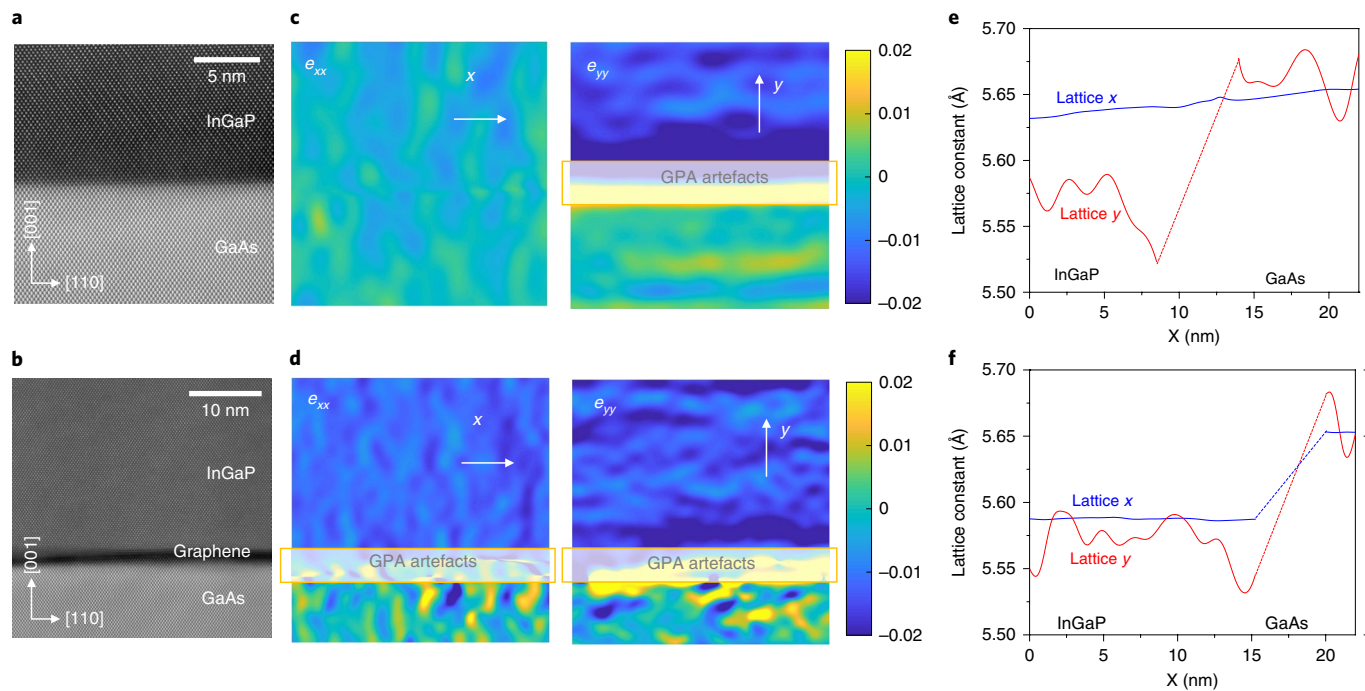
Fig. 2 | Cross-sectional ADF-STEM images of InGaP grown on bare GaAs and graphene/GaAs. a, ADF-STEM image of InGaP grown on bare GaAs. **b**, ADF-STEM image of InGaP grown on monolayer graphene-coated GaAs. **c**, Lattice mapping of InGaP grown on GaAs. The e_{xx} and e_{yy} refer to the difference between an InGaP lattice and a reference GaAs lattice (e_{xx} and e_{yy} = (InGaP lattice constant − GaAs lattice constant) / InGaP lattice constant, in the x and y directions, respectively). **d**, Lattice mapping of InGaP grown on graphene-coated GaAs. The colour-scale bars in **c** and **d** indicate the strain value. **e**, Lattice constant of InGaP on bare GaAs substrates along the x-axis. **f**, Lattice constant of InGaP on graphene-coated GaAs substrates along the y-axis. The lattice y line profiles include the noise inherent in the e_{yy} GPA maps, due to the limitations of GPA.

relaxation range). At a given average aspect ratio of heteroepitaxial InGaP (aspect ratio = 0.99) without graphene and heteroepitaxial InGaP (aspect ratio = 0.998) with graphene, obtained from the plot of the lattice constant from the GPA map in Fig. 2e,f, the % relaxation of InGaP with/without graphene is ~24% and 65–80%, respectively. These values are comparable to those obtained from the Raman analysis shown in Fig. 1. Note that some epilayers were slightly displaced from the graphene interface (Supplementary Figs. 5 and 6). Thus, both strain analysis and TEM investigation prove the existence of another relaxation pathway, other than the introduction of a dislocation, on graphene. This proof further suggests that, due to this alternative relaxation pathway, heteroepitaxy can be performed with a minimum involvement of threading dislocations, a process that has long been sought in the semiconductor community.

Considering the weakened interface between epitaxial films and substrates due to the existence of a graphene interlayer, one possible relaxation pathway would be through the weak epilayer–graphene interface. If the energy required to displace the bonding at the interface is weaker than that required to introduce a dislocation, the strain could be relaxed without introducing a dislocation. DFT corroborates our conclusion that interface displacement from one atomic site to the others on a slippery graphene surface can be a relaxation pathway, although the interaction still exists between the epilayers and substrates (Supplementary Fig. 7). The DFT calculation proves that the required energy for this interface displacement on a slippery graphene surface is an order of magnitude smaller than that required for the introduction of a dislocation or delamination (see details in Supplementary Information). Thus, a small strain built up in a heteroepitaxial film can be spontaneously relaxed on graphene. As shown in Fig. 3a,b, the calculated maximum energy barrier required for the interface displacement of the (001) InGaP epilayer on graphene-coated (001) GaAs is 37 mJ m^{-2} while the

calculated elastic energy required for introducing a dislocation is 635 mJ m^{-2} using dislocation theory[23], and that required for displacing the InGaP epilayer directly on GaAs substrates is 1,556 mJ m^{-2} (see details in Supplementary Information). Accordingly, the minimum energy required for the interface displacement on graphene is much smaller than the other critical energies required for strain relaxation, as summarized in Fig. 3b. This confirms that our observation on the relaxation of In$_{0.4}$Ga$_{0.6}$P epilayers on graphene even before the critical thickness for the introduction of a dislocation is reached is truly due to the spontaneous relaxation of strained epilayers on the slippery graphene surface[24]. We have calculated a critical thickness for spontaneous relaxation as a function of the epilayer thicknesses based on our modelling, considering the accumulated strain energy (see Supplementary Information)[25]. As shown in Fig. 3c, in the range of misfit strain that allows epitaxial growth (up to ~4%), spontaneous relaxation precedes the introduction of a dislocation. As the curve suggests, a few monolayers of III–V epilayers can be spontaneously relaxed, and a monolayer of epilayer can be immediately relaxed, on graphene with a misfit strain above ~3.5%. Thus, the introduction of a dislocation is not the major relaxation pathway on graphene surfaces. Since most heteroepitaxy occurs below that strain level, we expect that spontaneous relaxation will dominate the strain relaxation on graphene surfaces in heteroepitaxial systems, over the formation of dislocations.

To further clarify the above prediction, we performed heteroepitaxy of a highly lattice-mismatched system that is known to result in a high density of dislocations with conventional heteroepitaxial films. The expected outcome of spontaneous relaxation is to significantly reduce dislocations even for highly mismatched systems. To experimentally confirm this expectation, we grew 3.7% lattice-mismatched GaP on GaAs substrates with and without a graphene interlayer[26]. As predicted in our calculation shown in Fig. 3c, since
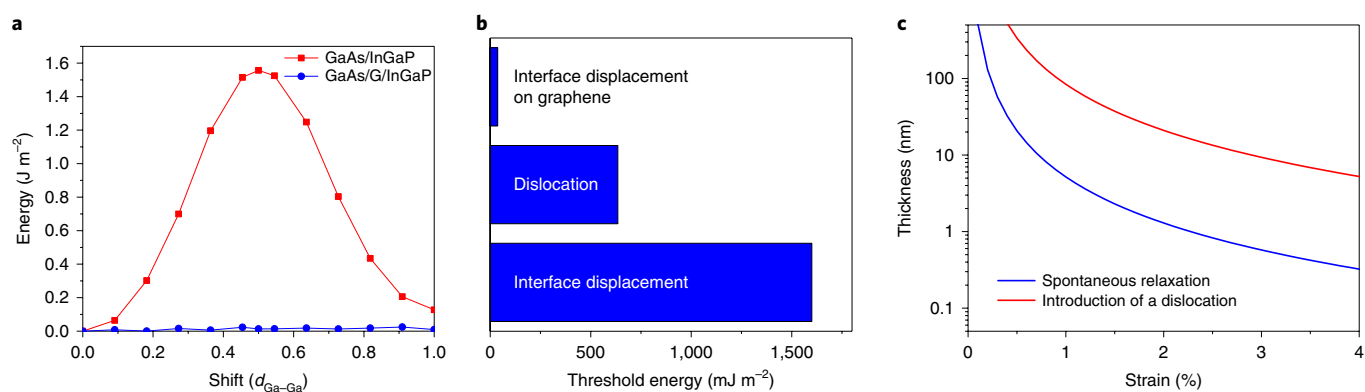
Fig. 3 | Theoretical calculation to understand spontaneous relaxation. a, Energy barrier required for the interface sliding of epilayers on graphene/ substrates and bare substrates. Interface sliding on graphene/GaAs needs only 37 mJ m⁻², while interface sliding on bare GaAs needs 1,556 mJ m⁻². **b**, Threshold energy for the situations of interface sliding on graphene (37 mJ m⁻²), the introduction of a dislocation (635 mJ m⁻²) and interface sliding on bare GaAs (1,556 mJ m⁻²). **c**, Critical thickness of a heteroepitaxy film with spontaneous relaxation.
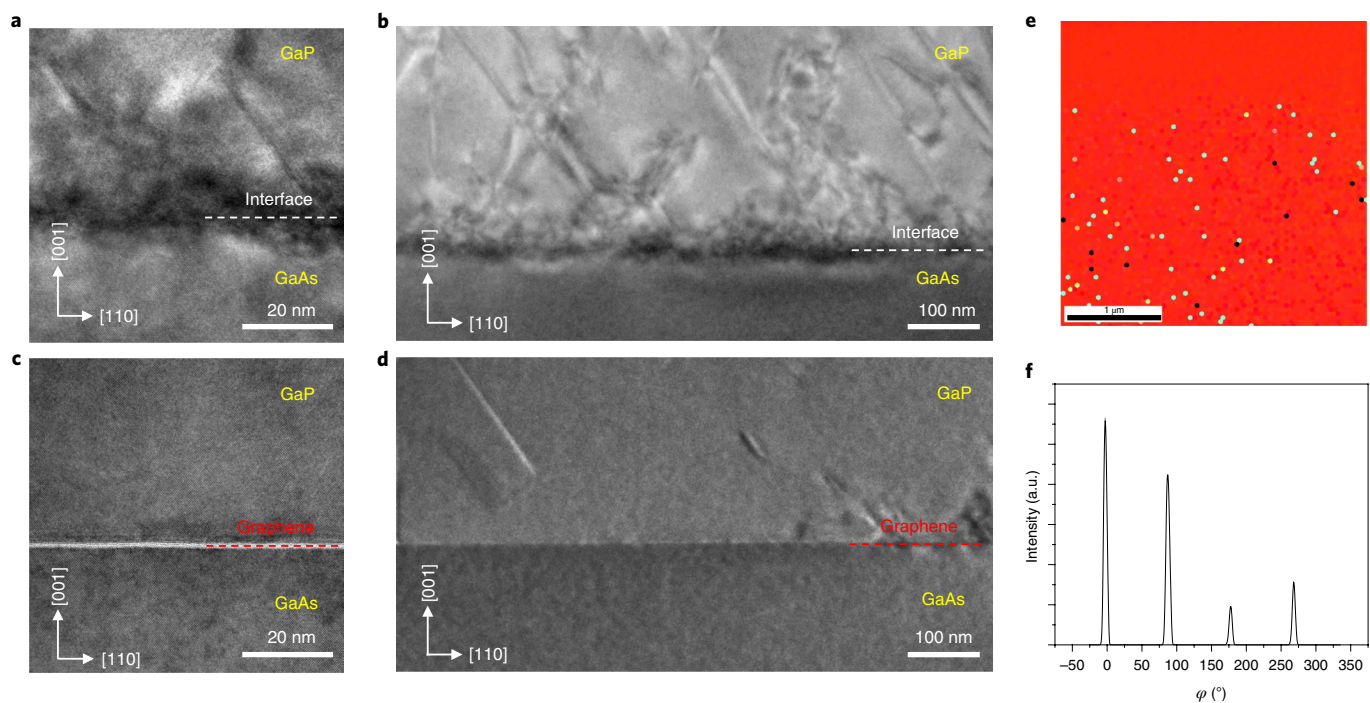

Fig. 4 | Highly mismatched system of GaP on GaAs. a–d, Cross-sectional view of GaP grown on bare GaAs (**a,b**) and cross-sectional view of GaP grown on graphene/GaAs (**c,d**), indicating the substantial reduction of dislocations via spontaneous relaxation on graphene/GaAs. **e**, EBSD plot of the exfoliated GaP epilayer. **f**, HRXRD azimuthal off-axis φ scan of the GaP epilayer.

the strain energy of a few monolayers of a fully strained GaP is already above the spontaneous relaxation limit, it is expected that spontaneous relaxation could still occur. Our TEM investigation on the epitaxial interfaces reveals that high-density dislocations with significant strain fringe are present near the conventional heteroepitaxial interface of GaP–GaAs (Fig. 4a,b and Supplementary Fig. 8). On the other hand, we observed a substantial reduction of dislocations at the interface with the heteroepitaxial interface of GaP–graphene–GaAs even with such a large lattice mismatch (Fig. 4c,d and Supplementary Fig. 8).

These findings clearly prove that the slippery graphene surface offers relaxation pathways other than by dislocations, via spontaneous relaxation, even for highly lattice-mismatched systems. As shown in Fig. 4a,c and Supplementary Fig. 9, cross-sectional TEM

images reveal a clear difference between GaP grown on bare substrates and that grown on graphene-coated substrates. A substantial reduction in threading dislocations was observed in the spontaneous relaxation case compared with the case of dislocation formation[27]. A plan-view ADF-STEM imaging analysis also confirmed the reduction of dislocations by spontaneous relaxation over a large area (see Supplementary Fig. 10). The counted dislocation density from our plan-view TEM investigation is 1.49×10^9 cm⁻² for heteroepitaxy on bare GaAs and 3.72×10^8 cm⁻² for heteroepitaxy on graphene-coated GaAs. Despite the reduction of dislocations, we still observed isolated defective areas having local strain and dislocations, which have to be dealt with to further improve the epilayer quality. For example, pinholes on graphene caused by a manual graphene transfer process must be avoided to prevent defect

formation through direct heteroepitaxy on the substrate, which creates local strain fields, causing dislocation formation. As shown in Supplementary Fig. 11, GaP on a graphene region shows a strain-free interface while GaP on a pinhole of the graphene shows strain fringes as well as dislocations. Defects such as stacking faults at the impinging points of spontaneously relaxed nuclei may not be avoided as nucleation sites cannot be digitally controlled to perfectly match the relaxed lattices of heteroepitaxial films; however, these defects may be alleviated by controlling the nucleation density or using guided nucleation via patterning. Finally, we mechanically exfoliated epitaxial GaP from graphene by applying a Ni stressor[28–30] to confirm that epitaxy mainly occurred on graphene-coated substrates; strong covalent bonds in conventional epitaxial films do not allow exfoliation[31,32]. We then performed electron backscatter diffraction (EBSD) scans on the exfoliated side of the GaP films. The EBSD map reveals the out-of-plane single crystallinity of GaP. The four-fold symmetry revealed by a high resolution X-ray diffraction (HRXRD) phi scan also confirms the in-plane single crystallinity of GaP (see Fig. 4e,f).

In summary, we report our discovery of an alternative pathway of relaxing misfit strain in heteroepitaxial films, other than by the formation of a dislocation, by growing on graphene-coated substrates. Theoretical analysis shows that the graphene surface has an extremely low energy barrier required for the interface sliding of epilayers. This enables spontaneous relaxation of the epilayer before the accumulated elastic energy created by the lattice mismatch induces misfit dislocations. From the system with a small lattice mismatch (InGaP on GaAs with 0.74% misfit), we observed that conventional heteroepitaxy gradually relaxes the misfit strain via the introduction of a dislocation, while heteroepitaxy on graphene-coated substrates abruptly relaxes the strain in the epilayer via interface displacement on the graphene's slippery surface. This effect becomes more prominent in a highly mismatched system (GaP on GaAs with 3.7% misfit), where a substantially reduced dislocation density is seen. Although avoiding localized sources that cause the nucleation of threading dislocations needs further investigation, the spontaneous relaxation technique reported here could enable the monolithic integration of largely lattice-mismatched systems with minimized dislocation density, which could eventually broaden the material spectrum for advanced electronics and photonics.

Online content

Any methods, additional references, Nature Research reporting summaries, source data, extended data, supplementary information, acknowledgements, peer review information; details of author contributions and competing interests; and statements of data and code availability are available at https://doi.org/10.1038/s41565-020-0633-5.

References

1. Chen, C. Q. et al. GaN homoepitaxy on freestanding (1100) oriented GaN substrates. *Appl. Phys. Lett.* **81**, 3194–3196 (2002).
2. Kwon, O. et al. Monolithic integration of AlGaInP laser diodes on SiGe/Si substrates by molecular beam epitaxy. *J. Appl. Phys.* **100**, 13103 (2006).
3. Matsunami, H. & Kimoto, T. Step-controlled epitaxial growth of SiC: high quality homoepitaxy. *Mater. Sci. Eng. R. Rep.* **20**, 125–166 (1997).
4. Vaisman, M. et al. Effects of growth temperature and device structure on GaP solar cells grown by molecular beam epitaxy. *Appl. Phys. Lett.* **106**, 063903 (2015).
5. Voigtländer, B., Weber, T., Šmilauer, P. & Wolf, D. E. Transition from island growth to step-flow growth for Si/Si (100) epitaxy. *Phys. Rev. Lett.* **78**, 2164–2167 (1997).
6. Luan, H.-C. et al. High-quality Ge epilayers on Si with low threading-dislocation densities. *Appl. Phys. Lett.* **75**, 2909–2911 (1999).
7. Currie, M. T., Samavedam, S. B., Langdo, T. A., Leitz, C. W. & Fitzgerald, E. A. Controlling threading dislocation densities in Ge on Si using graded SiGe layers and chemical-mechanical polishing. *Appl. Phys. Lett.* **72**, 1718–1720 (1998).
8. Andre, C. L. et al. Impact of dislocation densities on n+/ p and p+/ n junction GaAs diodes and solar cells on SiGe virtual substrates. *J. Appl. Phys.* **98**, 14502 (2005).
9. Lee, M. L., Antoniadis, D. A. & Fitzgerald, E. A. Challenges in epitaxial growth of SiGe buffers on Si (111), (110), and (112). *Thin Solid Films* **508**, 136–139 (2006).
10. Chen, R. et al. Nanolasers grown on silicon. *Nat. Photonics* **5**, 170–175 (2011).
11. Ebert, C. B., Eyres, L. A., Fejer, M. M. & Harris, J. S. Jr MBE growth of antiphase GaAs films using GaAs/Ge/GaAs heteroepitaxy. *J. Cryst. Growth* **201-202**, 187–193 (1999).
12. Lee, M. L., Fitzgerald, E. A., Bulsara, M. T., Currie, M. T. & Lochtefeld, A. Strained Si, SiGe, and Ge channels for high-mobility metal-oxide-semiconductor field-effect transistors. *J. Appl. Phys.* **97**, 1 (2005).
13. Bean, J. C., Sheng, T. T., Feldman, L. C., Fiory, A. T. & Lynch, R. T. Pseudomorphic growth of Ge_xSi_{1-x} on silicon by molecular beam epitaxy. *Appl. Phys. Lett.* **44**, 102–104 (1984).
14. Fitzgerald, E. A. et al. Totally relaxed Ge_xSi_{1-x} layers with low threading dislocation densities grown on Si substrates. *Appl. Phys. Lett.* **59**, 811–813 (1991).
15. Song, T. L., Chua, S. J., Fitzgerald, E. A., Chen, P. & Tripathy, S. Strain relaxation in graded InGaN/GaN epilayers grown on sapphire. *Appl. Phys. Lett.* **83**, 1545–1547 (2003).
16. Massies, J. & Grandjean, N. Oscillation of the lattice relaxation in layer-by-layer epitaxial growth of highly strained materials. *Phys. Rev. Lett.* **71**, 1411–1414 (1993).
17. Daruka, I. & Barabási, A.-L. Dislocation-free island formation in heteroepitaxial growth: a study at equilibrium. *Phys. Rev. Lett.* **79**, 3708–3711 (1997).
18. Kim, Y. et al. Remote epitaxy through graphene enables two-dimensional material-based layer transfer. *Nature* **544**, 340–343 (2017).
19. Kong, W. et al. Polarity governs atomic interaction through two-dimensional materials. *Nat. Mater.* **17**, 999–1004 (2018).
20. Li, X. et al. Large-area two-dimensional layered hexagonal boron nitride grown on sapphire by metalorganic vapor phase epitaxy. *Cryst. Growth Des.* **16**, 3409–3415 (2016).
21. Attolini, G. et al. Optical and structural characterization of LP MOVPE grown lattice matched InGaP/GaAs heterostructures. *Mater. Sci. Eng. B* **91-92**, 123–127 (2002).
22. Kato, T., Matsumoto, T. & Ishida, T. Raman spectral behavior of $In_{1-x}Ga_xP$ (0 < x < 1). *Jpn. J. Appl. Phys.* **27**, 983–986 (1988).
23. Lee, H. et al. Study of strain and disorder of $In_xGa_{1-x}P$/(GaAs, graded GaP) ($0.25 \leq x \leq 0.8$) using spectroscopic ellipsometry and Raman spectroscopy. *J. Appl. Phys.* **75**, 5040–5051 (1994).
24. King-Ning, T., Mayer, J. W. & Feldman, L. C. *Electronic Thin Film Science for Electrical Engineers and Materials Scientists* (Macmillan, 1996).
25. Matthews, J. W. & Blakeslee, A. E. Defects in epitaxial multilayers: I. Misfit dislocations. *J. Cryst. Growth* **27**, 118–125 (1974).
26. Freundlich, A., Bensaoula, A., Bensaoula, A. H. & Rossignol, V. Interface and relaxation properties of chemical beam epitaxy grown GaP/GaAs structures. *J. Vac. Sci. Technol. B* **11**, 843–846 (1993).
27. Morales, F. M. et al. Microstructural improvements of InP on GaAs (001) grown by molecular beam epitaxy by in situ hydrogenation and postgrowth annealing. *Appl. Phys. Lett.* **94**, 41919 (2009).
28. Bae, S.-H. et al. Unveiling the carrier transport mechanism in epitaxial graphene for forming wafer-scale, single-domain graphene. *Proc. Natl Acad. Sci. USA* **114**, 4082–4086 (2017).
29. Shim, J. et al. Controlled crack propagation for atomic precision handling of wafer-scale two-dimensional materials. *Science* **362**, 665–670 (2018).
30. Kim, J. et al. Layer-resolved graphene transfer via engineered strain layers. *Science* **342**, 833–836 (2013).
31. Bae, S.-H. et al. Integration of bulk materials with two-dimensional materials for physical coupling and applications. *Nat. Mater.* **18**, 550–560 (2019).
32. Kum, H. et al. Epitaxial growth and layer-transfer techniques for heterogeneous integration of materials for electronic and photonic devices. *Nat. Electron.* **2**, 439–450 (2019).

Methods

Graphitization, transfer, epitaxy and exfoliation with characterization.
Silicon sublimation was conducted on a Si-face (0001) 4H-SiC wafer with a 0.05°
miscut. After normal degreasing cleaning with acetone and isopropyl alcohol,
the SiC substrate was annealed at high temperature (850 °C) under high vacuum
($<1\times10^{-6}$ mbar) for 20 min to clean oxides from the SiC surface. Graphitization
followed at a higher temperature (1,550 °C) in an argon atmosphere, which can
suppress the Si sublimation rate. While maintaining the argon atmosphere, the
chamber was cooled and graphene formed on the SiC. Raman spectroscopy
with lateral resolution of 2 μm confirmed the quality of the graphene. The small
intensity of the D peak in the Raman data confirms that the graphene quality
is suitable for further experiment. The G to 2D ratio of the Raman spectrum of
graphene shows that monolayer graphene was obtained through our graphitization
process (Supplementary Fig. 1).

To peel off the graphene from the SiC substrates, a Ni stressor layer was
deposited on graphene/SiC with ~400 MPa stress. Since the adhesion between
Ni/graphene is stronger than that between graphene/SiC, the Ni/graphene was
exfoliated from the SiC using a thermal-releasing tape handler. The Ni/graphene was
immediately transferred to the GaAs substrates after HCl cleaning to remove oxides
on the GaAs surface. TFB nickel etchant was used to etch the Ni and leave graphene/
GaAs substrates. Raman spectroscopy confirmed the graphene's quality after the
transfer process. As shown in Supplementary Fig. 2, there is still no strong D peak,
which means that the transfer process did not cause severe damage on the graphene.

A close-coupled showerhead vertical metalorganic chemical vapour deposition
(MOCVD) reactor was used to grow InGaP and GaP on the graphene-coated
GaAs (001) and bare GaAs (001) substrates. Nitrogen was used as a carrier gas,
and the reactor pressure was kept at 100 torr during the growth. First, the reactor
temperature was ramped up to the growth temperature with an arsine supply to
prevent substrate desorption. Next, the growth of InGaP and of GaP was carried
out using trimethylindium, trimethylgallium and phosphine as precursors. The
V/III flow-rate ratio was 255 for InGaP and 149 for GaP, and the growth
temperature was 650 °C for both InGaP and GaP. After the growth, the reactor
was cooled to 300 °C under phosphine overpressure.

We used Raman spectroscopy and TEM on the InGaP and GaP epilayer grown
both on graphene-coated GaAs and on GaAs to understand the spontaneous
strain-relaxation phenomenon. Then, we exfoliated the epilayer grown on the
graphene-coated substrates to confirm that most of the surface area of the GaAs
was covered with graphene. EBSD and HRXRD were used on the exfoliated surface
to confirm the crystallinity of the epilayer grown at the interface.

Electron microscopy. Plan-view scanning electron microscopy was conducted
using a FEI Helios 660 and a Zeiss Merlin high-resolution scanning electron
microscope. To characterize the samples using the cross-sectional TEM, samples
were protected by amorphous carbon films deposited by electron beam at an
early stage and sequentially polished by the FEI Helios 660 with 30 kV, 5 kV and
2 kV to minimize Ga ion contamination. TEM images and selected area electron
diffraction (SAED) patterns were obtained using a JEOL ARM 200cF operated
at 200 kV and a FEI Titan operated at 120 kV. For ADF-STEM images, the beam
convergence angle was ~25 mrad, with a probe current of ~10 pA. The acquisition
time was 6 μs per pixel, and we summed ten frames. High-resolution TEM images
were used without a post-filtering process.

GPA was conducted to measure the strain field between the substrate and
target films based on high-resolution electron microscope images. The GPA had
a 0.01% strain resolution[33]. We used DigitalMicrograph with the GPA plugin
developed by Humboldt-Universität zu Berlin[34].

Data availability

The data that support the findings of this study are available from the
corresponding author upon reasonable request.

References

33. Han, Y. et al. Sub-nanometre channels embedded in two-dimensional
    materials. *Nat. Mater.* **17**, 129–133 (2018).
34. Hÿtch, M. J., Snoeck, E. & Kilaas, R. Quantitative measurement of
    displacement and strain fields from HREM micrographs. *Ultramicroscopy* **74**,
    131–146 (1998).

Acknowledgements

Author contributions

J.K., S.-H.B., K. Lu, Y.H., S.K. and K. Lee conceived the experiment. S.-H.B., K. Lu and H.K.
contributed to the epitaxial growth. S.-H.B., K. Lu, B.-S.K., C.K. and J.S. worked on the
graphene transfer. Y.H. and S.K. performed the TEM. S.-H.B., K. Lu, Y.H., S.K., D.A.M.,
K. Lee and J.K. analysed the TEM data. K.Q., W.K. and Y.B. analysed the Raman spectra.
C.C. and Y.N. designed and performed the DFT calculation. B.-S.K. and J.L. contributed to
the modelling data summary and figure configuration. K. Lu, H.S.K. and P.C. performed
XRD. K. Lu and H.K. carried out the EBSD measurement. S.-H.B., K.Q., J.P., M.J. and J.K.
contributed to the strain relaxation analysis. All the authors contributed to the discussion
and analysis of the results regarding the manuscript. J.K. directed the team.

Competing interests

The authors declare no competing interests.

Additional information

Supplementary information is available for this paper at https://doi.org/10.1038/
s41565-020-0633-5.

Correspondence and requests for materials should be addressed to K.L. or J.K.

Reprints and permissions information is available at www.nature.com/reprints.